SUPPLEMENTARY INFORMATION

Supplementary note 1

Maxwell's laws dictate that the electrical polarization of a cell is an unavoidable consequence of a cell being an intact compartment separated from the environment by thin membrane structures. The membrane acts as a barrier to the flow of ions driven by the applied electric field, and the charge carriers accumulate at the interfaces and give rise to an induced polarization. If the applied field is nonuniform in space, then the cell will move because the field acting on accumulated ions in different regions of the polarized cell will be unequal. This motion is called dielectrophoresis (DEP), which importantly can be used to manipulate electrically *neutral* matter. In this regard DEP is distinct from the phenomenon of electrophoresis that describes the motion of any electrically *charged* entity in either a uniform or nonuniform electric field. A first-order approximation of the time-averaged DEP force experienced by an electrical polarized spherical cell may be written as [31]:

$$\langle F_{DEP} \rangle = \frac{1}{4} V \varepsilon_m \mathrm{Re}\left[\tilde{K}_{CM}\right] \nabla |E|^2$$

where V is the cell volume, ε_m is the relative permittivity of the suspending fluid, E is the root-mean-square amplitude of the electric field, and ∇ is the gradient operator. The direction of motion due to DEP is governed by K_{CM}, the complex polarizability of a spherical particle, which may be mathematically represented as,

$$K_{CM} = \left(\frac{\tilde{\varepsilon}_p - \tilde{\varepsilon}_m}{\tilde{\varepsilon}_p + 2\tilde{\varepsilon}_m} \right)$$

where $\tilde{\varepsilon}$ is the complex permittivity, which depends on the relative permittivity ε_r, the permittivity of free space ε_0, the conductivity σ, and the frequency of the applied electric field ω according to the expression $\tilde{\varepsilon} = \varepsilon_r \varepsilon_0 - j\sigma/\omega$. The subscripts "p" and "m" denote the particle (or cell) and medium, respectively. The direction of the DEP force is governed by the real part of the Clausius-Mosotti factor $\left(\mathrm{Re}\left[\tilde{K}_{CM}\right]\right)$, which may be considered as a dielectric contrast between the cell and its suspending medium. If then cell is more electrically polarizable than the suspending medium $\left(\tilde{\varepsilon}_p > \tilde{\varepsilon}_m\right)$, then the dielectric contrast is positive and the cell is pulled toward field maxima located at the edges of microelectrodes by positive DEP (pDEP). Conversely, if cells are less electrically polarizable than the suspending medium, the dielectric contrast is negative and cells are repelled from microelectrode edges by negative DEP (nDEP). The cytoelectric properties of biological cells, embodied in the effective permittivity of the particle $\tilde{\varepsilon}_p$, emerge from the properties of the cell interior, the cell shape and size, the characteristics of the diffuse ionic atmosphere surrounding cells, as well as the structure and composition of biomembranes.

For erythrocytes, the plasma membrane separates the cell interior from the suspending medium and presents a barrier to the flow of ions, giving rise to the accumulation of charge at the membrane/electrolyte interface. A mathematical model for layered nonspherical particles like erythrocytes was previously developed to predict and rationalize the effect moment along each semiaxes [60]. To a first approximation, the biconcave shape of an erythrocyte may be modeled as a lossy dielectric oblate ellipsoid surrounded by a thin, electrically insulating shell representing the plasma membrane (figure S1).

The effective complex anisotropic permittivity of the cell along the major axes (x- and z-directions) may be written,

$$\tilde{\varepsilon}_{p,z} = \tilde{\varepsilon}_{mem} \left[\frac{\tilde{\varepsilon}_{cyt} + \Delta_z \left(\tilde{\varepsilon}_{cyt} - \tilde{\varepsilon}_{mem}\right)/a}{\tilde{\varepsilon}_{mem} + \Delta_z \left(\tilde{\varepsilon}_{cyt} - \tilde{\varepsilon}_{mem}\right)/a} \right]$$

Where Δ_z is the thickness of the membrane, a is the semiaxes of the internal ellipsoid, and $\tilde{\varepsilon}_{mem}$ and $\tilde{\varepsilon}_{cyt}$ are the complex permittivities for the cell membrane and the cytosol, respectively. The complex permittivity of the cell about the minor semiaxes (y-direction) can be computed by the same expression using Δ_y and b. The complex polarization factor for the ellipsoidal particle along the x- and z-directions is given by,

$$K_{CM,z}(\omega) = \frac{\tilde{\varepsilon}_{p,z} - \tilde{\varepsilon}_m}{3\left[\tilde{\varepsilon}_m + \left(\tilde{\varepsilon}_{p,z} - \tilde{\varepsilon}_m\right) L_{\parallel}\right]}$$

where $L_{\parallel}$ is the depolarization factor along the x- and z-coordinates, defined by the elliptical integral as $L_{\parallel} = \frac{a^2 b}{2(a^2-b^2)}\left[\frac{\pi/2}{\sqrt{a^2-b^2}} - \frac{b}{a^2}\right]$. $L_{\perp}$ is the depolarization along the short semi-axis b and is calculated from $L_{\perp} = 1 - 2L_z$.

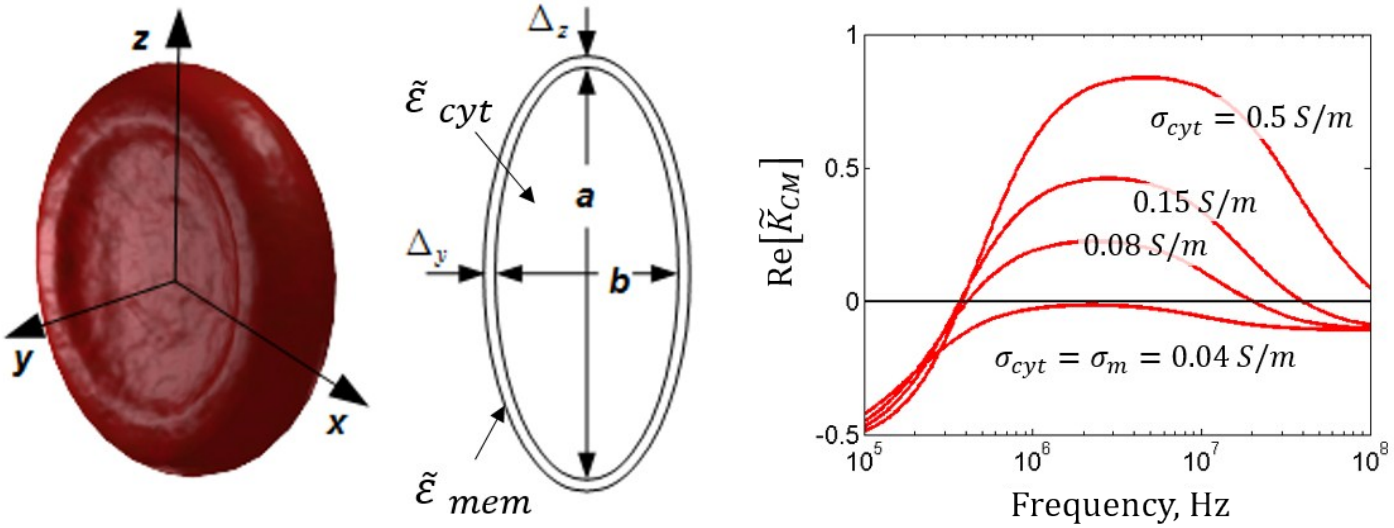

Supplemental figure 1: Dielectric shell model for human erythrocyte. (Left) Illustration of an erythrocyte with the defined coordinate system used in the dielectric shell model. (Middle) A cross-sectional view in the yz-plane of a layered oblate ellipsoid used to model the biconcave shaped cell. The membrane thickness has been exaggerated for clarity. (Right) The predicted DEP behavior of the cell is plotted as a function of the frequency of the applied field for varying values of the cytosolic conductivity.

Previous dielectric measurements of human blood cells report cell interior permittivity values that are comparable to that of water ($\varepsilon_{cyt} \approx 57\varepsilon_0, \varepsilon_m \approx 78\varepsilon_0,$) and the internal conductivity of a sealed erythrocyte is about $\sigma_{cyt} = 0.5\ S/m$ [63]. Therefore, the DEP behavior of erythrocytes is strongly dependent upon the contrast between the conductivity of the cell interior σ_{cyt} and that of the suspending medium σ_m. Indeed, from these considerations, it follows that a particle having an interior compartment with a conductivity $\sigma_{cyt} \gg \sigma_m$ may be captured by energizing the electrodes by a DEP signal having a frequency f greater than the particle crossover frequency f_{XO}. Generally, biological cells that are viable and/or functional tend to have internal compartments and are able to actively maintain physiological ionic concentrations as well as sealed membranes that retain these ions while suspended in a medium having low ionic conductivity. As a result, structurally intact, functional cells can usually be captured by positive DEP forces when the electrical conductivity of the internal compartment is sufficiently high compared to the suspending medium or $\sigma_{cyt} \gg \sigma_m$ and $f > f_{XO}$.

Biological cells that are not viable and/or functional tend to lose ions from their internal compartments when they are suspended in a medium having low ionic conductivity [36]–[38] This is often the result of ion leakage through their membranes, and given sufficient time, $\sigma_{cyt} \rightarrow \sigma_m$. The average of the particle polarizabilities along the semiaxes is plotted as a function of the frequency of applied electric field in figure S1 for different values of cytoplasmic conductivities to illustrate the effect of ion leakage from the cell interior. The shell model predicts that if the conductivity of the interior compartment of the particle is substantially similar to that of the particle suspending medium then $\tilde{K}_{CM} \rightarrow 0$ and the particle will experience a significantly weakened polarization, and hence a weakened DEP force. Polarizability spectra of an erythrocyte predicted by the dielectric shell model (**supplemental figure 1**) are consistent with observations of the DEP behavior of erythrocytes following exposure to the ionophore monensin. The decrease in cytosolic conductivity relates to the leakage of ions into the suspending medium. The predicted shift in the cross-over frequency (the frequency where $Re[\tilde{K}_{CM}] = 0$) toward lower frequency values matches what was observed experimentally.

Supplementary note 2

The concentration distribution of solute within the microdialysis channel was mathematically modeled to understand operational limitations and to optimize design parameters. At low Reynold's numbers, the fluid flow profile is laminar and the two layers do not mix [39]. Ions diffuse quickly across the liquid-liquid interface within the narrow channel and therefore can be rapidly depleted from the specimen stream (**supplemental fig 2A**). Net transport of ions is driven across

the microchannel by diffusion while bulk fluid flow dominates transport of ions downstream. To understand how this affects conductivity, we need only to model ion transport in a two-dimensional plane parallel to the length of the channel (figure 2A). The concentration distribution C_i of ion *i* in space and time can be written

$$D_i\frac{\partial^2 C_i}{\partial x^2}+D_i\frac{\partial^2 C_i}{\partial y^2}=\frac{\partial C_i}{\partial t}+u(y)\frac{\partial C_i}{\partial x}$$

where D is the diffusion coefficient. Assuming laminar flow is fully established within the microchannel, the velocity distribution between the microchamber top and bottom can be written as $u(y)=6\bar{u}\frac{y}{H}\left(1-\frac{y}{H}\right)$ where H is the chamber height and $\bar{u}$ is the mean fluid velocity. The ratio of the diluent to sample flow rates sets the final ionic concentration at the device outlet, provided sufficient time is allowed for ions to diffuse across the microfluidic channel. The simulations predicted that there is a critical mixing length needed to reduce the ion concentration to a target level. Importantly, that critical length is independent of the ratio of specimen to diluent flow rates (**supplemental fig 2B)**.

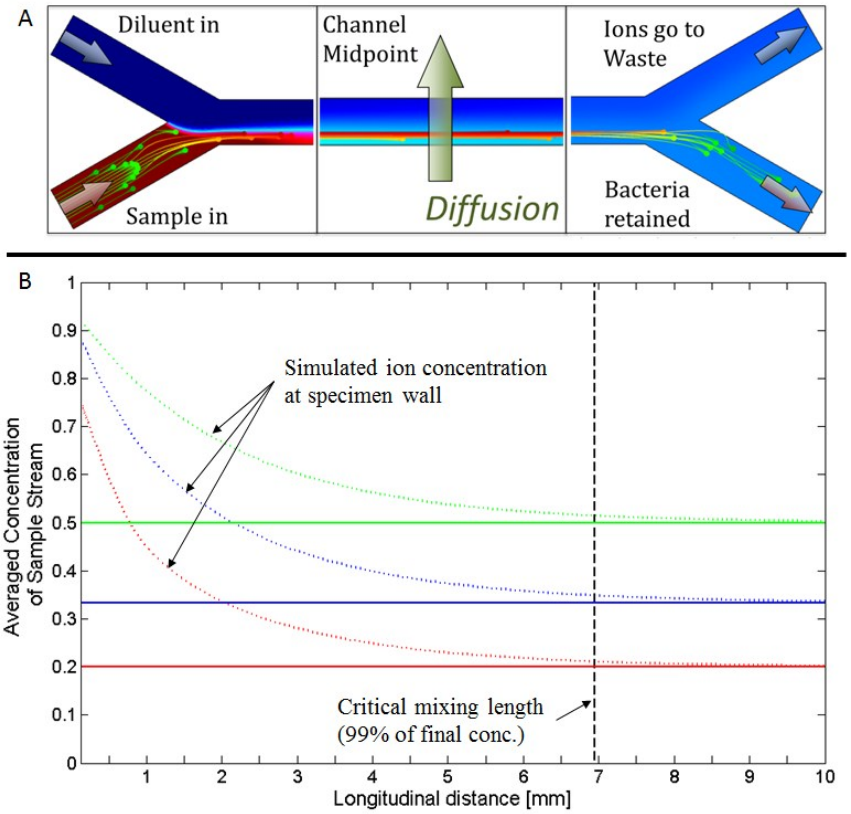

Supplemental figure 2 Simulations of ion transport within the microfluidic membraneless dialysis device. (A) Schematic of an "H-filter" microfluidic device used to deionize a bacterial suspension. Under appropriate conditions the sample and diluent fluids intersect at a three-way junction and flow down the separation channel side-by-side. Ions diffuse down the concentration gradient across the fluid interface into the diluent flow streams. Bacteria remain in the sample stream and exit the chamber at the lower right outlet. (B) Simulated transport of low molecular weight solutes within the microfluidic H-filter device when the specimen flow rate is half (green curve), one-third (blue curve) and one-fifth (red curve) of the total flow. In each simulation, the average flow velocity in the mixing channel was the same.

The mean time taken for fluid of average velocity $\bar{u}$ to travel length L of the chamber $is\ t=L/\bar{u}$. Einstein showed that the root-mean-square distance a particle diffuses in time *t* along a single dimension is related to the diffusion coefficient *D* by $\langle x^2\rangle=2Dt$ [40]. Assuming that diffusion downstream in the microchannel is negligible compared with the bulk fluid velocity, the length required for full mixing of the solute can then be written as $L_{mix}=\frac{\bar{u}H^2}{D}=\frac{HQ_{total}}{WD}$ [41], [42]. This expression provides a design guide and highlights the geometrical criteria important for achieving efficient dialysis by passive diffusion at high sample processing rates. A precision CNC mill was used to fabricate micromolds to cast microdialysis devices (**Supplementary fig. S3A and S3B)**. The mold was designed with a high-aspect ratio ribbed structure

to define a microdialysis channel 3 mm in height, 10 cm in length, and 250 µm in width. The channel was angled at the fluid inlets and outlets to encourage fluid to spread evenly throughout the width of the channel before the diluent and specimen streams converged and split at the Y-junctions.

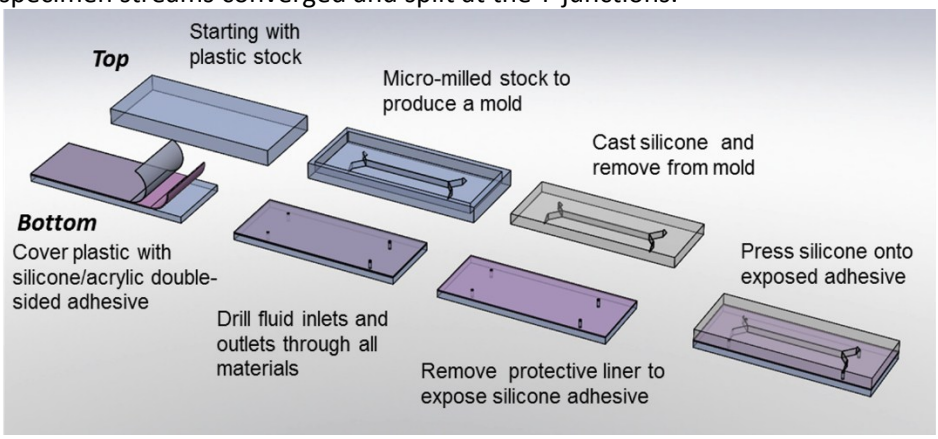

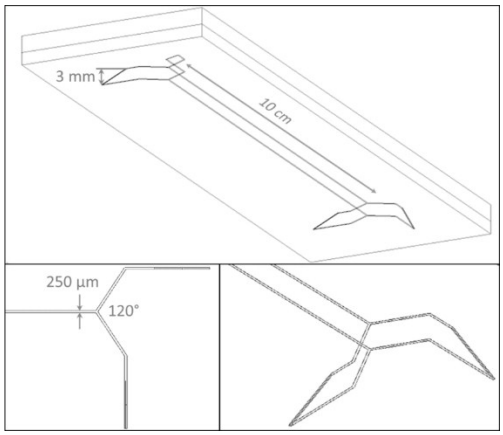

Supplementary figure 3 Overview of the microfluidic membraneless dialysis device. (Left) The upper path shows how micro-milling is used to produce high-aspect ratio features that define the channel in a plastic mold. Silicone is cast in the mold to form the microfluidic chamber top and side walls. The lower path explains how the microfluidic device bottom is made. A double-sided differential silicone/acrylic adhesive sheet is laminated onto an acrylic sheet and fluid ports are drilled through the composite. The silicone cast is bonded to the base to produce the final device. (Right) The top image is an isometric view of a wireframe diagram of the micromilled mold used to form a high-aspect ratio microchannel in silicone. In the lower left a top view of the wireframe diagram showing the microscale dimension (250 µm) over which rapid diffusion of ions occurs. In the lower right is a zoomed in view of the angled entrance structure that helps to ensure fluid streams are injected and withdrawn evenly over the entire height of the microchannel.

The membraneless microdialysis design presented herein resembles the well-known "H-filter" micromixer [41]. In the H-filter design the diluent and specimen stream intersect and split at right angles. This creates a stagnation point that causes the two streams to mix. An important difference is that the membraneless dialyzer incorporated an angled entrance flow profile which is less than 180˚. This facilitated laminating and splitting fluid layers. In operation, a diluent fluid with low ion concentration is fed into one inlet of a MMD and layered over a thin specimen fluid stream, which enters through a separate inlet (**supplemental Fig 4A**). The hydrodynamic resistance of the two outlet ports was balanced to achieve the desired volumetric splitting ratio (**supplemental Fig. 4B**).

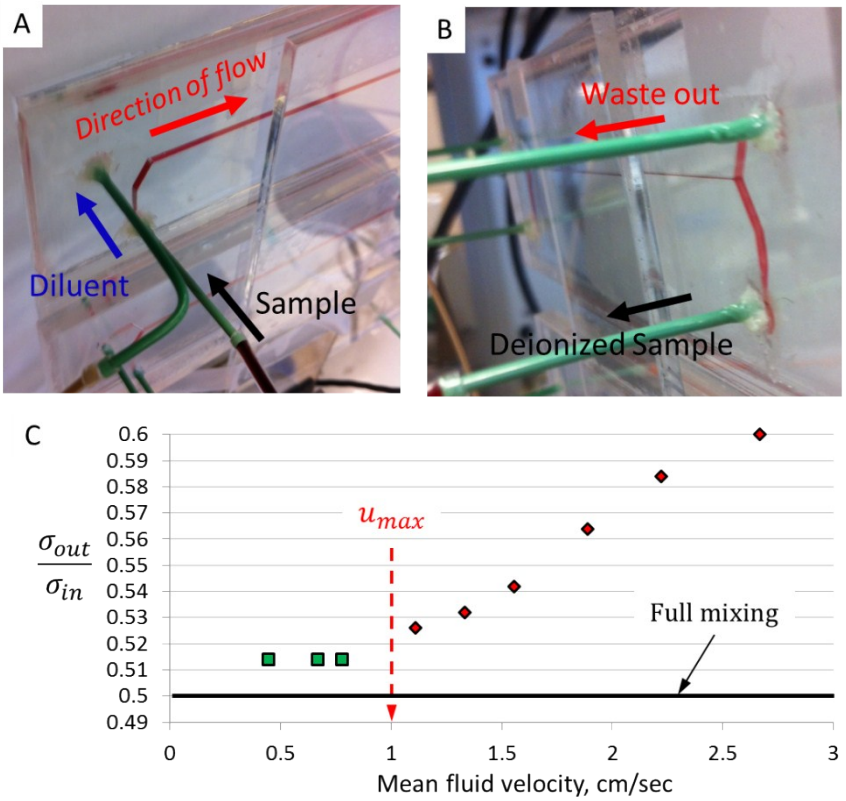

Figure 4: Experimental evaluation of the microfluidic membraneless dialysis device. (A) Photograph shows a saponin-treated blood sample being continuously injected into the bottom inlet of the dialysis device. Clear diluent is also being pumped into the top inlet. (B) Photograph showing the waste stream (red arrow) and sample stream (black arrow) at the outlet bifurcation point of the membraneless microdialysis device. (C) The measured conductivity reduction for a single microfluidic dialysis device for increasing mean fluid flow velocities. The horizontal black line at 0.5 shows the expected ratio for complete mixing and the vertical broken red line is the theoretical mean velocity limit that allows for complete mixing.

To evaluate the performance of the MMD, the electrical conductivity of the specimen was measured at the sample outlet for different average flow velocity values and compared to the initial conductivity to compute a concentration reduction factor (**supplemental fig. 4C**). The critical average flow velocity that allowed for complete mixing of sodium ions across the channel by passive diffusion was estimated to be 1 cm/sec. Operating at fluid flow rates below this critical value reduced the electrical conductivity level of the test solution by nearly one-half, which is in accordance with simulation data. Operating below this predicted maximum average fluid velocity resulted in full deionization of the specimen stream.